Design of Broad-Beam Microstrip Reflectarray

PIYAPORN KRACHODNOK AND RANGSAN WONGSAN
School of Telecommunication Engineering, Institute of Engineering
Suranaree University of Technology
111 University Avenue, Muang District, Nakhon Ratchasima, 30000
THAILAND
Email: priam@sut.ac.th

Abstract: - The reflectarray's elements arrangement for generating an arbitrary phase distribution in the antenna aperture and thus a wide beamwidth of the far field pattern is presented. The desired phase delay of reflectarray elements, which duplicated the same radiating aperture as backscatters, is determined on the construction of the curvature of a shaped backscatter surface with the help of Snell's law for beam forming to cover a broad area. The Method of Moments (MoM) and the infinite-array are applied to calculate reflection phase characteristics. The phase and radiation pattern synthesis method for microstrip reflectarray that has to illuminate a predefined circular area are presented by using a variety of discretization of elementary geometrical functions such as, triangular, quadratic, circular, gaussian, cosine, squared cosine, and parabolic distributions. These backscatter functions are discussed in terms of merits and demerits to find appropriate radiation characteristics such as radiation pattern, -3 dB beamwidth, and maximum gain for utilization in Wireless Local Area Network (WLAN) application. The optimized feed distance is calculated from the aperture efficiency by considering feed blockage efficiency and the influence of the feed position on the -3 dB beamwidth and gain performance has been investigated. Having confirmed the validity of this approach, the X-band antenna prototype is designed and developed. This reflectarray is tested experimentally and shows good performance.

Key-Words: - reflectarray, phase array, broad-beam antenna

1 Introduction

The characteristics of antennas (performance, technology, and cost) are an important issue in wireless communication systems. The shaped-beam antenna for satellite communication was first developed to give approximately uniform coverage of the earth [1]-[2]. Recently, the similar requirement but different application; that is, the indoor high speed data transmission: Wireless Local Area Networks (WLAN) operating in the millimeter wave, again has attracted considerable attentions [3]-[7]. Especially, the large-scale indoor base station of such system requires the wider-beam antenna for covering an effectively broad area. Therefore, the widely circular beam antenna is an alternative for WLAN applications as shown in Fig.1. The required important feature is the transmitted power that has to be efficiently distributed over the coverage whereas, outside the coverage, the field strength has to fall off rapidly. In [5], Smulders *et al*. presented the design of a 60 GHz shaped reflector antenna for WLAN access points by using backscatter reflector, which was fabricated from the modified parabolic surface. From this design, the backscatters have been fabricated from the circular metal sheet that their surfaces are shaped to be geometric curvature. In case of WLAN systems, such antennas are improper because their structures suffer from mechanical drawbacks such as bulkiness and the need for an expansive custom mold for each coverage specification.

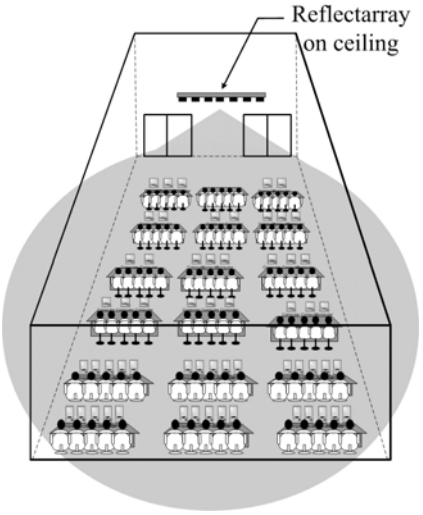

Fig. 1 Reflectarray for WLAN large-scale indoor base station.

A microstrip reflectarray that combines some of the best feature of microstrip arrays and parabolic reflector was presented in [8]-[14]. The reflectarray antenna consists of a flat reflecting surface and an illuminating feed as shown in Fig.2. On the reflecting surface, there are many isolated elements (e.g. printed patches, dipoles, or rings), which array on flat printed circuit broad (PCB) without any power division transmission lines. A reflectarray configuration is attractive because it allows a single mechanical design to be used repeatedly for a wide variety of different coverage specifications without the need for expensive fabrication of a new mold. The only changes require that the printed reflecting element dimensions can be changed for each design in order to generate the different beams. Thus, many of the high recurring costs associated with shaped reflector antennas can be eliminated with flat printed reflectarray [11]. The flat geometry of a reflectarray also lends itself to easier placement and deployment on the WLAN large-scale indoor base station and also in terms of manufacture. In addition, a flat printed reflectarray fulfils the antenna requirements for low profile and light weight.

In this paper, we propose the design techniques of a wide-beam microstrip reflectarray antenna using discretization of elementary geometrical functions to synthesize the appropriated curvature for forming a wide-beam pattern of reflectarray. An effective technique for optimum reflectarray design depend on the aperture efficiency by considering feed blockage efficiency and the influence of the feed position on the -3 dB beamwidth and gain performance has been investigated. To achieve such broad-beamwidth, phase of each array element in the reflectarray antenna is designed specifically to emulate the curvature of the backscatter function by using patches of different sizes [11].

In the first section, we will present the general design approach as far as it involves the reflection phase characteristic (Section 2) that describes the desired phase delay of reflectarray elements and the phase calibration technique by using a full-wave method of moment and the infinite-array. In Section 3, we apply this approach to calculate the radiation pattern of the proposed antenna. Design considerations of broad-beam microstrip reflectarray and experimental results are described in Section 4. Finally, the conclusions are given in Section 5.

2 Reflection Phase Characteristic

2.1 Geometrical functions of backscatter

The geometry of a reflectarray antenna, which duplicated the same radiating aperture as curved backscatter reflector, fed with a feed antenna is illustrated on Fig. 2. The distributions of backscatter curvature using the geometrical function are shown in Table 1. Where D is assumed to be the diameter and A is the depth of the backscatter reflector, respectively. The results of these functions will be taken to find required phase delay and radiation pattern.

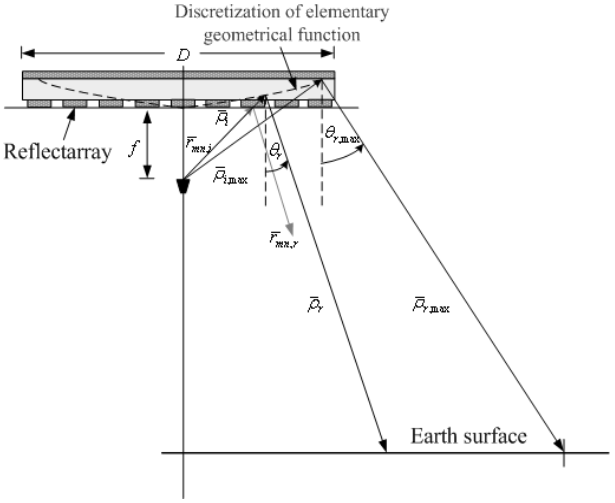

Fig. 2 Synthesis model of broad-beam microstrip reflectarray.

Table 1 Formulations of elementary geometrical functions.

Backscatter Shapes	Formulations
Circular	$f(z') = A\sqrt{1-\left(\frac{2}{D}z'\right)^2}$
Gaussian	$f(z') = Ae^{-(\frac{2}{D}z')^2}$
Quadratic	$f(z') = A\left(1-\left(\frac{2}{D}z'\right)^2\right)$
Parabolic	$f(z') = z'^2/4f$
Cosine	$f(z') = A\cos(\frac{\pi}{D}z')$
Squared cosine	$f(z') = A\cos^2\left(\frac{\pi}{D}z'\right)$
Triangular	$f(z') = A\left(1-\frac{2}{D}\lvert z'\rvert\right)$

With a given standard X-band horn as shown in Fig. 3, the appropriate distance between the horn and the center of reflectarray can be estimated by considering the spillover and taper efficiencies

relations given in [14]. At optimum value of aperture efficiency, a feed distance to diameter ratio (*f/D*) provides spillover and taper efficiencies of 76% and 84%, respectively. Thus, feed distance is chosen to be of 21.25 cm at 10λ reflector diameter. This structure radiates the beam that illuminates a predefined circular area without substantial spatial variation.

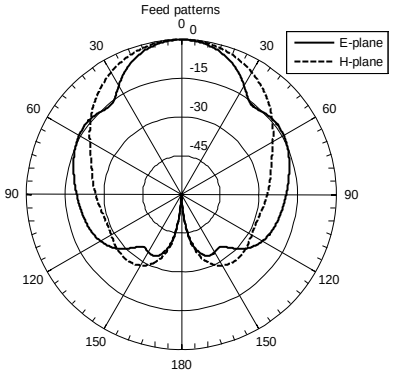

Fig. 3 Radiation pattern of standard X-band horn.

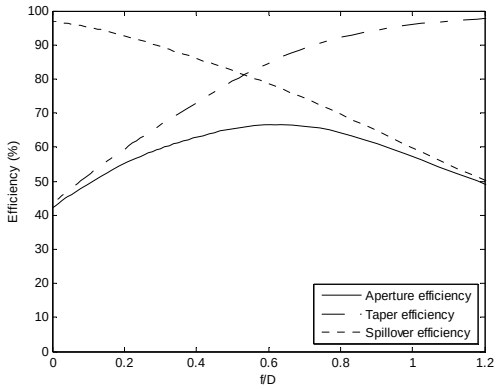

Fig. 4 Reflectarray efficiency.

2.2 Required Phase Delay

Fig. 2 illustrates the incidence of wave on the surface of an analysis model of printed microstrip reflectarray, which parameters used in this figure are described below:

$\vec{r}_{mn,i}$ the vector from the feed to the *mn*-th reflectarray element, which can be obtained by using flat geometry;

$\vec{r}_{mn,r}$ the reflected vector from the reflectarray surface to far-field;

$\vec{\rho}_i$ the vector from the feed to the shaped reflector surface, which can be obtained by using curvature geometry;

$\vec{\rho}_r$ the reflected vector from the shaped reflector surface to far-field;

θ_i incidence angle;

θ_r reflection angle;

D dimension of the reflector;

f distance between the feed and the center of the reflectarray.

In general, the feed may be positioned at distance from the reflectarray. The path lengths from the feed to all reflectarray elements are all different, which lead to different phase delays. In this paper, the desired phase delay is determined on the construction of the curvature of a shaped backscatter surface with the help of Snell's law. The relations of the microstrip reflectarray surface to the shape of backscatter are two coordinate systems in this figure: one describes the coordinates (x_r, y_r, z_r) of the reflectarray and the other describes the coordinate (x_b, y_b, z_b) of the backscatter. The selected shaped reflector is determined by using functions of elementary geometric $(f(z'))$ that aperture cross sections of all backscatters are confined to be circular, same diameter, and very small radius of point source. Since the reflectarray is designed, the following coordinate is used to find the point on the backscatter surface at a given patch element position on the reflectarray as given by (1).

$$\begin{aligned} x_b &= x_r + \left| f(z') - z_r \right| \tan\theta_i \cos\phi_i, \\ y_b &= y_r + \left| f(z') - z_r \right| \tan\theta_i \sin\phi_i, \end{aligned} \tag{1}$$

where the phase center of the feed is located at $(0,0,0)$ and the incidence angle can be described in terms of geometrical dimensions

$$\theta_i = \tan^{-1}\left[\frac{\sqrt{x_r^2 + y_r^2}}{f}\right], \tag{2}$$

$$\phi_i = \tan^{-1}\left[\frac{y_r}{x_r}\right]. \tag{3}$$

The total path length from the feed to the reflectarray aperture is the sum of the distance from the feed to a point on the backscatter surface and the distance from that point to the corresponding point on the reflectarray with the rays satisfying Snell's law on the backscatter surface. In the analysis of backscatter, it is desirable to find a unit vector that is normal to the local tangent at the surface reflection point

$$\hat{n} = \frac{\nabla\left[z - f(z')\right]}{\left|\nabla\left[z - f(z')\right]\right|}. \tag{4}$$

With the help of Snell's law of reflection, the reflected angle for the backscatter can be expressed in (5).

$$\theta_r = 2\cos^{-1}\left[-\frac{\vec{\rho}_i}{|\vec{\rho}_i|}\cdot\hat{n}\right]-\theta_i. \quad (5)$$

The differential path length (ΔL_{mn}) and the phase delay ($\Delta\Phi_{mn}$) for the *mn*-th reflectarray element are given by

$$\Delta L_{mn} = |\vec{\rho}_i| + \frac{z_b - f}{\sin\theta_r} - |\vec{r}_{mn,i}|, \quad (6)$$

$$\Delta\Phi_{mn} \text{ in degree} = \left[(1-N)k_0\Delta L_{mn}\right]\frac{360}{2\pi}, \quad (7)$$

where N is integer. The above indicates that the compensating phase can be repeated every 360 deg, and the portion that is an integer multiple of 360 deg can be deleted.

The required aperture phase delays of all elements are calculated and will be used to design the dimension of the reflectarray elements as shown in Fig.5. These phase delays are duplicated the same radiating aperture as shape of backscatter. To compensate these phase delays, the elements must have corresponding phase advancements designed.

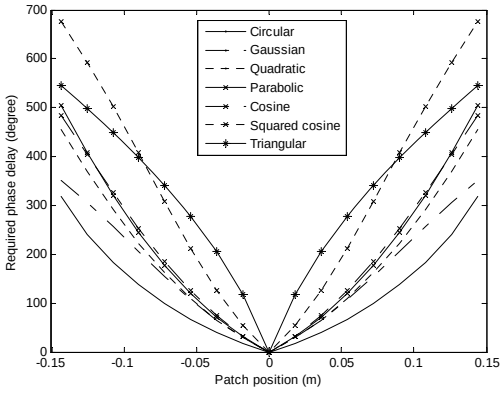

Fig. 5 Desired phase delay synthesis for reflectarray elements using geometrical functions.

2.3 Element Characterization

The most important and critical segment of the reflectarray design is its element characterization. To compensate for above phase delays, the elements must have corresponding phase advancements designed. Its phase change versus element change (patch size, etc.) must be calibrated correctly. If the element design is not optimized, it will not scatter the signal from the feed effectively to form an efficiently far-field beam. Also in this paper, the phase calibration technique uses a full-wave method of moment and the infinite-array approach to model the effect of the finite grounded dielectric substrate underlying the single radiator [12],[14].

In order to determine the solution used to design and analyze a microstrip reflectarray, we assume an incident plane wave with an electric field of the form

$$\bar{E}^{inc} = \bar{E}_0 e^{-jk_0(xu_i+yv_i-zw_i)}, \quad (8)$$

where the complex vector $\bar{E}_0$ defines the amplitude and direction of the incident field and

$$u_i = -\sin\theta_i\cos\phi_i,\ v_i = -\sin\theta_i\sin\phi_i,\ w_i = -\cos\theta_i. \quad (9)$$

The phase reference for this and the following fields are at the bottom of substrate. In the absence of array elements, the reflected field from the dielectric substrate and ground plane can be expressed as

$$\begin{bmatrix} E_\theta^{ref} \\ E_\phi^{ref} \end{bmatrix} = \begin{bmatrix} R_{\theta\theta} & 0 \\ 0 & R_{\phi\phi} \end{bmatrix}\begin{bmatrix} E_{0\theta} \\ E_{0\phi} \end{bmatrix} e^{jk_0(xu_i+yv_i-z\cos\theta_i)} = \bar{\bar{R}}\cdot\bar{E}_0 e^{jk_0(xu_i+yv_i-z\cos\theta_i)}, \quad (10)$$

where $R_{\theta\theta}$ and $R_{\phi\phi}$ are the plane wave reflection coefficients as given in [14].

The presence of the elements gives rise to an additional scattered field component given by

$$\begin{bmatrix} E_\theta^{scat} \\ E_\phi^{scat} \end{bmatrix} = \begin{bmatrix} S_{\theta\theta} & S_{\theta\phi} \\ S_{\phi\theta} & S_{\phi\phi} \end{bmatrix}\begin{bmatrix} E_{0\theta} \\ E_{0\phi} \end{bmatrix} e^{jk_0(xu_i+yv_i-z\cos\theta_i)} = \bar{\bar{S}}\cdot\bar{E}_0 e^{jk_0(xu_i+yv_i-z\cos\theta_i)}. \quad (11)$$

Evaluation of the total scattered field from the microstrip reflectarray is based on the assumption that each element of the finite reflectarray scatters as a Huygens source with reflection coefficient equivalent to the total reflection coefficient of an infinite array of similar elements.

$$\bar{E}^{tot} = \begin{bmatrix} R_{\theta\theta}+S_{\theta\theta} & S_{\theta\phi} \\ S_{\phi\theta} & R_{\phi\phi}+S_{\phi\phi} \end{bmatrix}\begin{bmatrix} E_{0\theta} \\ E_{0\phi} \end{bmatrix} e^{jk_0(xu_i+yv_i-z\cos\theta_i)}. \quad (12)$$

From (12), the reflection phase required for the design to compensate above phase delays can be found from the result of this result.

The scattering coefficients ($\bar{\bar{S}}$), defined in (11), are found by using a full-wave solution. The method of moment impedance matrix for infinite array of uniform elements can be computed as

$$Z_{ij} = -\frac{1}{s^2}\sum_{m=-\infty}^{m=\infty}\sum_{n=-\infty}^{n=\infty}\tilde{J}_i(k_x', k_y')\cdot\bar{\bar{G}}(k_x', k_y')\cdot\tilde{J}_j(k_x', k_y') \quad , \quad (13)$$

where s is center-to-center elements spacing in both x and y directions, $\tilde{J}$ is the Fourier transform of the ith expansion mode current, and $\bar{\bar{G}}$ is the dyadic Green's function for the dielectric substrate.

The voltage vector elements can be expressed in (14)

$$V_i = \bar{J}_{s0}\cdot\bar{\bar{G}}(k_0u_i, k_0v_i)\cdot\bar{J}_i(k_0u_i, k_0v_i), \quad (14)$$

where

$$\bar{J}_{s0} = \frac{-2}{\eta_0}\begin{bmatrix}\hat{x}(E_{0\theta}\cos\phi_i - E_{0\phi}\cos\theta_i\sin\phi_i)\\ +\hat{y}(E_{0\theta}\sin\phi_i - E_{0\phi}\cos\theta_i\cos\phi_i)\end{bmatrix}. \quad (15)$$

Fig. 6 shows simulated results of reflection phase of infinite array. The obtained results indicated that, if the element size L is excessively small, either the reflection phase cannot be made to cover the full required 0° to 360° phase range, or it changes excessively fast around the element resonance. This available phase shift rang is limited by the reflectarray antenna bandwidth (around 4%).

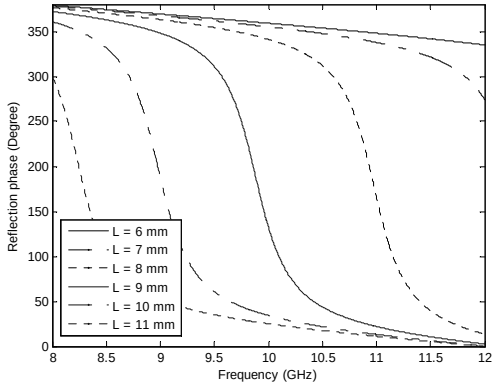

Fig. 6 Reflection phase of total reflected field from an infinite array of microstrip patches.

3 Radiation Pattern Synthesis

With the compensating phases of all elements known, the far-field radiation patterns can be calculated by the conventional array theory [13], where the radiations of all elements are summed together below. Considering a planar array consisting of $M \times N$ elements that are nonuniformly illuminated by a low-gain feed, the reradiated field from the patches in an arbitrary direction, $\hat{u}$, will have the form

$$E(\hat{u}) = \sum_{m=1}^{M}\sum_{n=1}^{N}F(\vec{r}_{mn}\cdot\hat{a}_z)\cdot A(\vec{r}_i\cdot\hat{u}_r)\cdot A(\hat{u}\cdot\hat{u}_r), \quad (16)$$
$$\cdot\exp\left[-jk_0\left(|\vec{r}_{mn}| + \vec{r}_i\cdot\hat{u}\right) - j\Delta\Phi_{mn}\right],$$

where F is the feed pattern function, A is the reflectarray element pattern function, $\vec{r}_i$ is the vector from the centre of reflectarray to mn-th element, $\hat{u}_r$ is the unit vector of reflected field, and $\Delta\Phi_{mn}$ is the required compensating phase of the mn-th element calculated by (7).

The calculated results that indicate the different radiation patterns for various geometrical functions are shown in Fig.7. The steepness of the pattern edges and the angular positions of these edges confirm that the antenna efficiently illuminates the target area to be covered (±65°). Radiation patterns are different due to phase of reflectarray elements which are duplicated the same radiating aperture as backscatter. Because of phase change versus element change, each reflectarray type (as backscatter shapes) provides different characteristics such as -3 dB beamwidth (HPBW) and relative power, reported in Table 2.

From Table 2, it is observed that the HPBW of seven backscatter reflectarray types are different. For average consideration, it is apparent that the squared cosine has the widest beamwidth and is followed, in order, by gaussian, cosine, quadratic, parabolic, and circular, which are 166°, 164°, 156°, 150°, 140°, and 133°, respectively, while HPBW of triangular is about 27° on each main beam. Since the relative power is strongly coincided with the HPBW i.e., the narrower the beamwidth the higher the relative power and vice versa. However, reflection surface for reflectarray elements, which are synthesized in this paper, are placed position near centre of shaped backscatter. Thus, the circularly geometrical function yields the highest relative power and followed, in order, by parabolic, gaussian, triangle, quadratic, cosine, and squared cosine, respectively.

From all the aforementioned radiation characteristics, it can be summarized that these reflectarrays can be chosen according to the characteristic requirements in practicable applications. For example, if the widest HPBW for large coverage area is required, then, the geometric function of squared cosine should be the best choice. But its advantage, which should be concerned, is the highest ripple level. However, if we need a very high gain reflectarray antenna, the circularly geometrical function should be applied. From view graphs of radiation patterns in Fig.7, it is

easy to find the proper geometrical function at which meets the requirement of the characteristic specifications. To get more advantages in one characteristic while sacrificing the merit of another characteristic in the same backscatter function is difficult to avoid.

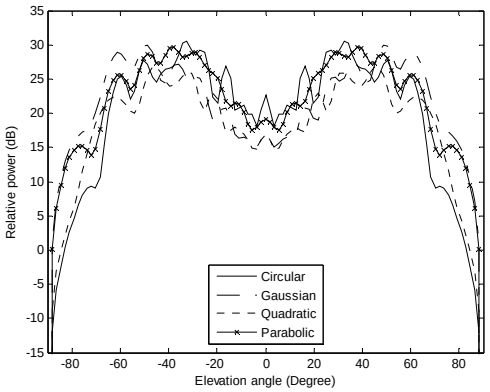

(a)

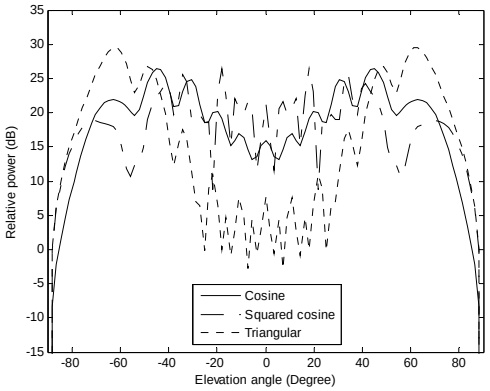

(b)

Fig. 7 H-plane radiation pattern synthesis for microstrip reflectarray.

Table 2. Characteristics of reflectarray with various geometrical types.

Backscatter Shapes	HPBW (degree)	Maximum relative power (dB)
Circular	133	30.29
Gaussian	164	28.49
Quadratic	150	25.58
Parabolic	140	28.87
Cosine	156	24.27
Squared cosine	166	22.01
Triangular	27	28.06

4 Design Considerations of Broad-Beam Microstrip Reflectarray and Experimental Results

As an example, authors clinch to choose compensating phase of reflectarray elements with the parabolic backscatter function because it has appropriate characteristics, i.e. low ripple level, high relative power (high gain), and wide HPBW (wide coverage area). To verify the theoretical calculation, the reflectarray prototype is fabricated at the operating frequency of 10 GHz. This frequency is chosen corresponding to the available equipment. The reflectarray of 30 cm dimension is designed and measured with a standard X-band horn feed, which is placed in front of reflectarray surface. The cell elements of reflectarray are printed on a TACONIC substrate with thickness 0.762 mm and permittivity ε_r = 2.33. The centre-to-centre elements spacing is fixed at a distance $s = 0.6\lambda_0$ in both x and y directions.

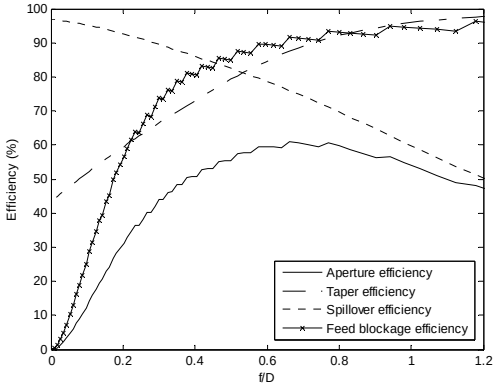

Fig. 8 Reflectarray efficiency by considering the feed blockage efficiency.

It is easy to calculate efficiency for a feed horn pattern and reflectarray due to illumination taper and spillover as given in [13],[14]. However, there are several other factors that can significantly reduce efficiency. Because the feed horn and its supporting structures are in the beam direction of the reflectarray, therefore, some part of the radiation is blocked. Also, considering the aperture, taper, spillover, and feed blockage efficiencies relations versus distance between the feed and the reflectarray to a dimension (*f/D*) ratio are calculated and plotted in Fig. 8. As in the case of front feed reflector, there is an optimum value of *f/D* that maximizes aperture efficiency for a given feed pattern. This maximum value is slightly lower than the optimum aperture efficiency for the parabolic case because of a slightly lower taper efficiency.

When the feed blockage efficiency is considered, maximum aperture efficiency is reduced and feed distance is changed while a reflectarray dimension is fixed. In this paper, we have investigated the influence of the feed position on the -3 dB beamwidth (HPBW) and gain performance before the reflectarray is fabricated. Where the first feed distance f is located at the point that maximizes aperture efficiency (61%).

In order to optimize the feed position of broad-beam reflectarray, the calculated results as shown in Fig. 9 indicate the different radiation patterns for the various feed positions. The total reradiation field is computed as the summation of all the contributions from each array element. The prescribed field requirements have been satisfied by an appropriate choice of the radiating patches selected from the complex design curves obtained in the analysis stage.

Table 3 Characteristics of reflectarray.

Feed distance	HPBW (degree)	Gain (dBi) @ θ = 0°	Maximum gain (dBi)
f - 10% f	158	1.43	8.81
f - 5% f	151	-6.13	9.35
f	144	0.32	10.75
f + 5% f	144	1.99	11.10
f + 10% f	145	1.52	12.16

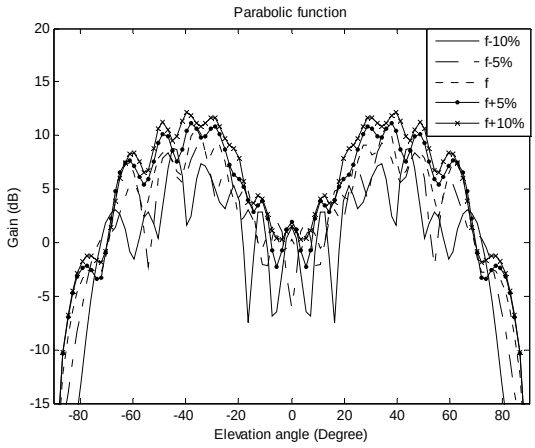

Fig. 9 Radiation pattern in H-plane of broad-beam reflectarray for the various feed positions.

The steepness of the pattern edges and their angular positions confirmed that the antenna efficiently illuminates the target area to be covered (±65°). The obtained radiation patterns are different due to phase of reflectarray elements, which duplicated the same radiating aperture as parabolic backscatter. Moreover, the ripple appeared on the top of each pattern can indicate that if the feed distance is reduced, then the ripple is increased. Away from the main beam, the phase center may move around and appear as multiple points, as stray reflections and surface currents affect the radiation pattern. Because of the phase change versus element change, each feed distance provides different characteristics such as HPBW and gain, which are reported in Table 3.

From Table 3, it is found that the HPBW of reflectarrays is different when the feed distance is varied. For average consideration, it is apparent that the feed position not far away in distance from reflectarray provides the widest beamwidth. Since the maximum gain is strongly coincided with the HPBW, i.e., the narrower the beamwidth the higher the maximum gain and vice versa. However, the position of reflection surface for reflectarray elements is placed near the centre of backscatter. Thus, the enlargement of the feed distance yields the lowest feed blockage efficiency and the highest gain at θ = 0°.

However, it is generally observed that when the antenna beam is enlarged, the antenna gain is reduced. With the optimum design requirement, the feed distance is chosen at 25 cm, which caused the maximum aperture efficiency to be reduced by approximately 2% but its gain is increased. In Fig. 10, the prototype of reflectarray antenna is realized following this approach and measured. From the measurement as shown in Fig. 11, the antenna has the HPBW of 145° and maximum gain of 13 dB at the frequency of 10 GHz. The measured gain patterns have been corrected by 2 dB for loss in the waveguide feed transition. An additional cause of asymmetry observed in the patterns is fabrication tolerance. The computed performances of this reflectarray are in accordance with those of the measured prototype. However, the measured and computed radiation patterns taken along the strut show a relatively much larger ripple of almost 3 dB in amplitude.

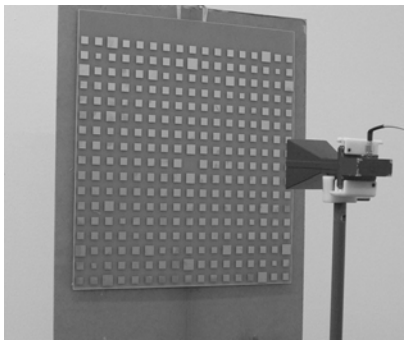

Fig. 10 Reflectarray prototype.

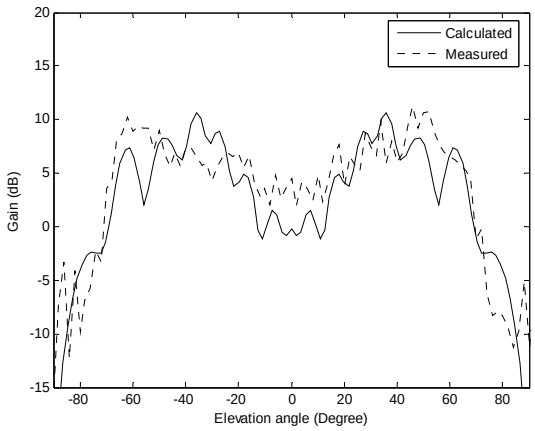

Fig. 11 Calculated and measured radiation patterns of designed reflectarray at 10 GHz.

5 Conclusion

In this paper, we have investigated a theoretical approach to design a reflectarray antenna usable of WLAN applications. The reflectarray can be chosen according to the characteristic requirements in practicable applications by using the synthesis of phase and radiation pattern of various reflectarray types. The optimized feed distance is calculated from the aperture efficiency by considering feed blockage efficiency and the influence of the feed position on the -3 dB beamwidth and gain performance has been investigated. The simulation of this reflectarray demonstrates that increasing feed distance can enhance maximum gain but its HPBW is reduced. From all the aforementioned radiation characteristics, it can be summarized that if we need to improve gain performance for broad-beam reflectarray antenna, an optimum feed distance would provide a feed radiation pattern which completely illuminates the reflectarray with minimal spillover. A test antenna built according to our model is in agreement with our expectations both in regards to coverage and maximum gain. The data show that flat reflectarrays can also give a defined footprint as a conventional antenna but without the complicated tooling and other drawbacks inherent in the latter.

References:

[1] S.G. Hay, D.G. Bateman, T.S. Bird, and F.R. Cooray, Simple Ka-band Earth coverage antennas for LEO satellites, *IEEE Antennas Propag. Soc. Int. Symp.*, Vol.1, 1999, pp.11-16.

[2] A.D. Olver, P.J.B. Clarricoats, A.A. Kishk, and L. Shafai, ed., *Microwave Horns and Feeds*, IEEE, New York, 1994.

[3] T.S. Bird, J.S. Kot, N. Nikolic, G.L. James, and S.J. Barker, Millimeter-wave antenna and propagation studies for indoor wireless LANs, *Antennas Propag. Soc. Int. Symp.*, Vol.1, 1994, pp.336-339.

[4] C.A. Fernandes and J.G. Fernandes, Performance of lens antennas in wireless indoor millimeter-wave applications, *IEEE Trans. Microwave Theory Tech.*, Vol.47, No.6, 1999, pp.732-737.

[5] P.F.M. Smulders, S. Khusial, and M.H.A.J. Herben, A shaped reflector antenna for 60-GHz indoor wireless LAN access points, *IEEE Trans. Veh. Technol.*, Vol.50, 2001, pp.584-591.

[6] R. Sauleau, P. Coquet, K. Shinohara, J. P. Daniel, N. Hirose, and T. Matsui, Millimeter wave antennas with gaussian radiation patterns, IEICE Trans Commun., Vol.E84-B, No.9, 2001, pp.2395-2406.

[7] A. Kumar, Antennas for wireless indoor millimeter-waves applications, *Proc. IEEE CCECE*, Vol.3, 2003, pp.1877-1880.

[8] R.E. Munson, H.A. Haddad, and J.W. Hanlen, Microstrip reflectarray for satellite communications and RCS enhancement or reduction, *U.S. patent 4 684 952*, 1987.

[9] D.C. Chang and M.C. Huang, Multiple-polarization microstrip reflectarray antenna with high efficiency and low cross-polarization, *IEEE Trans. on Antenna and Propag.*, Vol.43, No.8, 1995, pp. 829-834.

[10] J.A. Encinar, Design of two-layer printed reflectarrays using patches of variable size, *IEEE Trans. Antennas and Propag.*, Vol.49, 2001, pp.1403-1410.

[11] D.M. Pozar, S.D. Targonski, and R. Pokuls, A shaped-beam microstrip patch reflectarray, *IEEE Trans. Antenna and Propag.*, Vol.47, Issue 7, 1999, pp. 1167-1173.

[12] P. Krachodnok and R. Wongsan, Design of microstrip reflectarray antenna using backscattering technique, *Proc. of ITC-CSCC 2006*, Vol. 3, 2006, pp. 513-516.

[13] J. Huang, Analysis of a microstrip reflectarray antenna for microspacecraft applications, *The Telecommunications and Data Acquisition Progress Report 42-120*, 1995, pp. 153-173.

[14] D.M. Pozar, S.D. Targonski, and H.D. Syrigos, Design of millimeter wave microstrip reflectarray, *IEEE Trans. Antenna and Propag.*, Vol.45, No.2, 1997, pp. 287-296.

[15] P. Krachodnok and R. Wongsann, Optimum design of broad-beam microstrip reflectarray, *Proc. the 11th WSEAS International Conference on COMMUNICATIONS*, 2007, pp. 121-126.